



Energy and environmental analysis of a solar evacuated tube heat pipe integrated thermoelectric generator using IoT

Sakthi Priya Manivannan¹ · Divya Laxmi Gunasekaran¹ · Gowthami Jaganathan² · Shanthy Natesan² · Sabari Muthu Muthusamy² · Sung Chul Kim³ · Balaji Kumar¹ · Ganesh Kumar Poongavanam³ · Sakthivadivel Duraisamy¹

Received: 7 December 2021 / Accepted: 18 March 2022 / Published online: 31 March 2022
© The Author(s), under exclusive licence to Springer-Verlag GmbH Germany, part of Springer Nature 2022

Abstract

This paper investigates the solar evacuated tube heat pipe system (SETHP) coupled with a thermoelectric generator (TEG) using the internet of things (IoT). The TEGs convert heat energy into electricity through the Seebeck effect that finds application in the waste heat recovery process for the generation of power. The present work deals with the theoretical study on solar evacuated tube heat pipe integrated TEG and it is validated experimentally using with and without parabolic trough concentrating collector. However, it is found that the maximum power output due to the influence of the parabolic trough concentrator results in increased efficiency when compared with the non-concentrating SETHP-TEG system. Thus, the thermoelectric generator's electrical energy efficiency for the concentrating system was 0.151% greater than the latter one. A power electronic boost converter may enhance the acquired TEG output power to a maximum of 5.98 V. This would be directly used for both mobile charging and lighting applications in distant places and military camps where the community lacks sufficient electrical access. And the carbon credit of the TEG system is determined to find its potential in the environmental aspects of carbon emission per watt, carbon mitigation, and carbon credit and its results are 2.34×10^{-3} g/W, 0.027 tonnes, and 0.681 dollars respectively for a TEG module. Besides, the recorded real sensor data with Arduino is implemented in the experimental process for automatic remote monitoring of the temperature.

Keywords Solar evacuated tube heat pipe · Thermoelectric generator · Parabolic trough concentrating collector · Environmental analysis · Internet of things · Boost converter

Abbreviations

Al	Aluminum
CHP	Combined heat and power
DC	Direct current
DNI	Direct normal irradiance
HTF	Heat transfer fluid

ICT	Information and communication technology
IDE	Arduino Integrated Development Environment
IoT	Internet of things
PTC	Parabolic trough collector
SETHP	Solar evacuated tube heat pipe
STEGs	Solar thermoelectric generators
TE	Thermoelectric technology
TEC	Thermoelectric coolers
TEG	Thermoelectric generators
ZT	Figure of merit

Sung Chul Kim and Sakthivadivel Duraisamy contributed equally to this work.

Responsible Editor: Philippe Garrigues

✉ Ganesh Kumar Poongavanam
selgan.cad@gmail.com

- ¹ School of Mechanical Engineering, Vellore Institute of Technology, Vellore, Tamil Nadu 632014, India
- ² Kongu Engineering College, Erode, Tamilnadu 638060, India
- ³ School of Mechanical Engineering, Yeungnam University, 280 Daehak-Ro, Gyeongsan, Gyeongsbuk 712-749, Republic of Korea

Symbols

\$	Dollar (USD currency)
%	Percentage
A	Area of the heat pipe (m ²)
I_{max}	Maximum current for the corresponding ΔT value of TEG (A)
P_{max}	Maximum output power from the TEG (W)
Q_{in}	Heat input to the TEG (W)

V_{max}	Maximum voltage for the corresponding ΔT value of TEG (V)
V_o	Output voltage (volt)
V_{oc}	Open circuit voltage for the corresponding ΔT value of TEG (V)
$a_{tube-in}$	Absorptivity at absorber tube
$t_{tube-out}$	Transmissivity at the outer tube
η_{el}	Electrical energy efficiency of TEG (%)
η_{th}	Thermal efficiency of the SETHP TEG (%)
\pm	Tolerance/plus-minus
ΔT	Temperature difference of the TEG (K)
$^\circ$	Degree (angle)
A	Ampere
a	Dimensionless geometric parameter
Bi_2Te_3	Bismuth telluride
C	Capacitor
$^\circ C$	Degree celsius
CO_2	Carbondioxide
D	Duty ratio
E_{out}	Annual energy output (kWh/year)
H	Hour
I	Solar radiation (W/m ²)
I_s	Constant current input source
I_{sc}	Short circuit current for the corresponding ΔT value of TEG (A)
K	Kelvin
kg	Kilogram
kWh	Kilowatt-hour
L_{hp}	Length of the heat pipe (mm)
L	Inductance (H)
L_a	Domestic appliance loss
L_t	Transmission appliance loss
mm	Millimeter
N	No of thermocouples in setup
N	Life span (years) in environmental analysis
P_{out}	Output power from the TEG (W)
Q_c	Heat rejected by the cold junction of the TEG (W)
Q_h	Heat absorbed by the hot junction of the TEG (W)
R	The electrical resistance of the TEG (Ω)
R_L/R_o	External load ratio
S	Switching device
T_{cold}	The temperature at the cold junction of TEG (K)
T_{hot}	The temperature at the hot junction of TEG (K)
T_m	Mean operating temperature of TEG (K)
t	Thickness (mm)
V	Voltage/volt
V_{in}	Input voltage (volt)
V_{out}	Output voltage (V)
V_s	Constant supply voltage (volt)
W	Watt
W/m ²	Watt per meter square

A	Seebeck coefficient (V/K)
μA	Microampere
T	Thompson coefficient (V/K)
K	Thermal conductance of the TEG (W/K)
ρ	Electrical resistivity (Ωm)
ΔP	Change in power (W)
ΔV	Change in voltage (V)
ΔI	Change in current (A)
ΔR	Change in resistance (Ω)

Introduction

In today's world, one of the major concerns was to provide clean energy for a hazardous-free environment (Zoui et al. 2020). As of now, in the total energy consumption, about 80% is fossil fuel's contribution and the remaining is from other sources such as nuclear power, hydro, and renewable energy sources like solar, biofuels (Bildirici, 2018), wind, and geothermal energy (Faik Bilgili, 2020). But in the current state, fossil fuels are in the urge of depletion, and in the meantime, it is expected that due to the increase in the global population the electricity demand can be increased by 49% by the year 2040 (CAPP 2018). Furthermore, the use of fossil fuels leads to a rapid increase in greenhouse gas emissions, which has an impact on the world's long-term growth due to global warming, climate change, and other factors (Yousefi et al. 2016, Veronesi et al. 2017). Matching the gap between the depletion of fossil fuels and the growing population will lead us to depend on alternative fuels like renewable energy sources. One such renewable energy is solar which is of clean energy source and is feasible, and therefore it has a significant part in reducing the global crisis for energy. This kind of parabolic trough collector is a type of solar collector which could generate high temperatures with good efficiency. The performance of the system with bi-axial orientation and an absorber with a glass-covered enclosure is compared to mono- and bi-axial orientations without a glass-covered enclosure. In comparison to the situation of mono-axial orientation without a glass envelope, the useful daily energy gain raised by 33%, and the system's thermal efficiency improved by 8.9% in the design (Chargui et al. 2022). To achieve increased efficiency and to provide a combined effect, the power-generating PTCs are combined with different approaches. It is critical to achieving efficient PTCs with increased economic viability (Naveenkumar et al. 2021). The PTC thermal efficiency was tested at two distinct HTF flow rates of 0.005 kg/s and 0.033 kg/s with the adoption of two different phase change materials. The increased thermal efficiency of PTC without phase change material is 32% and with phase change material is 40.6% (Dhanapal et al.

2021). Scrap preheating combined with PTC saves the energy consumption by around 8% and also it is achieved 30% of minimum efficiency in the operation (Selvaraj et al. 2016). The performance of a small-scale solar concentrator — TEG system was investigated experimentally and aluminum foil is attached to the solar concentrating surface because of its great reflecting capacity (85%) and for its cost-efficient. To alter the receiver unit, a tiny fan with a TEG module was installed to remove the heat. The solar concentrator-TEG system's combined efficiencies with the TEG module and the solar concentrator module were found to be 0.23% and 0.63%, respectively (Verma et al. 2021). In this context, thermoelectric technology would also be a suitable energy source for the future as it directly converts the energy from one form to another without affecting the environment (Karthick et al. 2019). Thermoelectric (TE) technology is an eco-friendly technology that does not pollute any greenhouse gases and also has longer life since it has no moving parts (Ahiska and Mamur 2016). TE uses both the Seebeck (thermoelectric generators) and Peltier effect (thermoelectric coolers). In this, thermoelectric generators (TEGs) which work on the Seebeck effect converted to electrical energy from thermal energy (Verma et al. 2021). TEGs have superabundant advantages compared with other renewable energy devices as it is solid-state, clean energy conversion, cost-effective, and environmentally friendly (Enescu 2019). In addition to some conventional heat recovery applications, the heat pipe technology with solar concentrators would efficiently enhance the heat and mass transfer performance for cogeneration and one such is the hybrid solar water heating system with evacuated tube heat pipe along with the TEG and cooling jackets to produce combined heat and power (He et al. 2012; Lv et al. 2017; Ong et al. 2017). Typically, a cogeneration system produces electrical energy of 0.19 kWh and 300 l of hot water in a day at 55 °C for solar insolation below 1000 W/m². The obtained electrical power output is 64.80 W and the efficiency of the collector and electrical efficiency of thermoelectric modules are 47.54% and 1.59% respectively (Zhang et al. 2013). In this regard, the thermoelectric generator may be chosen due to advantages such as improved heat transfer characteristics on both sides of the thermoelectric generator due to the greater heat transfer area. TEGs are also used in the waste heat recovery system such as exhaust from the car for electricity generation and this helps in reducing fuel consumption. Heat pipes and TEGs can thus be employed in automobile applications due to their small size and solid-state nature (Orr et al. 2016). With increasing vehicle speed, which raises the hot junction temperature, the TEG's performance improves due to higher exhaust temperature, flow rate, and heat conduction via the TEG leg from the hot junction

(Yu et al. 2015). The nanostructured thermoelectric materials are used in flat-panel thermoelectric generators for achieving high performance (Kraemer et al. 2011). A comparison of the flat plate and annular thermoelectric generators was conducted, in this, the latter has attained higher heat transfer at standard solar radiation, and they have produced 1.92 W power output with an electrical efficiency of 2.63% (Manikandan and Kaushik 2016). While considering the materials for thermoelectric generators, bismuth telluride alloys are a suitable one and can maintain a maximum figure of merit at a temperature of 500 K (Goldsmid 2014) and can produce an electrical power of 14.1 W for hot and cold side temperatures of 250 °C and 50 °C respectively (Karabetoglu et al. 2012). Low convergence efficiency harms the growth of thermoelectric generators in the power generation sector, thus attention must be paid to the geometric configuration. The leg pin of thermoelectric generators can help enhance system efficiency by lowering thermal conductance (Ali et al. 2014). Likewise, if TEG's substrate area increases, then its output also increases as it increases the thermal concentration ratio and this was analyzed using ANSYS v12.0.1 (Chen et al. 2013). And the TEG performance was enhanced by the optimization of heat sink design using finite element numerical method and observed that the frontal area is increased by decreasing the length and this seems to be the best approach (Wang et al. 2012). The high rate of evaporation was attained by heat absorption in graphite plate fins and the magnetic field (Dhivagar and Mohanraj). To prevent heat loss and to retain heat, the exterior edge of the shell and coil condenser were filled with paraffin wax PCM (Mohanraj et al. 2021; Dhivagar and Kannan 2022). Many researchers were using different methods for better evaporation and condensation. In this article, PTC and aluminum heat sink is chosen for better evaporation and condensation of the heat pipe. None of the researchers have carried out the solar evacuated tube heat pipe with a heat sink attached at the condenser section of the heat pipe to produce the electricity. Furthermore, there have been no sufficient theoretical and experimental studies on TEGs utilizing a solar parabolic concentrator and without a concentrator. Thus theoretically and empirically, a TEG using SETHP with concentrator and without concentrator is examined in this paper. To monitor the temperature of the cold and hot sides of the TEGs, temperature sensors can be integrated with IoT for accuracy. Nowadays the role of Information and Communication Technology (ICT) has enhanced a lot with the emergence of IoT in every sector (Roziq et al. 2016). The significant thing with IoT is that it can easily collaborate as a part with any domain or application. The thermoelectric generator's progress using the IoT system helps in providing the sustainable power supply by the

integration of wireless sensor networks (Park et al. 2019). The IoT-based technology is used for monitoring and controlling double pipe heat exchanger (Sridharan et al. 2018) and observed that the temperature and mass flow can be measured without manpower by the way of creating channels and by collecting, analyzing, and visualizing data, acting on the data according to the required situation. This type of control system helps in continuous and appropriate operation. Since the voltage obtained from the system is low, and therefore it finds difficulty in the applications. And this can be managed by the usage of a DC-DC converter by boosting the output voltage (Park et al. 2019).

Thus, thermoelectric generators can be utilized as an alternative energy source since they are a green energy technology that can produce electricity from waste heat energy, lowering energy costs, reducing environmental impacts, and reducing the usage of fossil fuels. As a result, this technology has been identified as being vital in the heat recovery process as well as a viable alternative to the traditional method. The integration of IoT TEGs leads to a long-term power supply. The purpose of this article is to look into TEGs, which transfer heat energy from a SETHP with a concentrator and without concentrator system to electrical energy with the output being monitored by an IoT system and further the electrical output is boosted by the boost converter. The main theme of the present research is for investigating the energy and environment of the solar evacuated tube heat pipe integrated thermoelectric generator using IoT.

A monitoring system based on a low-cost microcontroller and IoT technique.

Experimental setup

The system comprises an individual evacuated tube heat pipe collector as shown in Fig. 1. It is exposed to sunlight equipped with two thermoelectric modules and cooling fans on the condenser part for the production of electricity. Solar evacuated tube heat pipe that is exposed to sunlight tends to absorb heat through copper heat pipe having the length of 1370 mm of the evaporator, adiabatic section, and 150 mm length of condenser section. The heat pipe is filled with low boiling working fluid such as ammonia -75 to 125 °C which has the best thermodynamic properties used to distribute heat across long distances for the entire heat pipe operation. The maximum amount of heat is absorbed in the evaporator followed by the adiabatic section. And the heat is conducted to the condenser region of the heat pipe which is coupled with the aluminum (Al) bars attached with TEG as shown in Fig. 1. The heat is then released through the heat spreader Al bar to the hot junction of thermoelectric modules and ejected at the cold junction. The TE module's cold side makes close contact with the Al fins cooling jacket, allowing airflow and heating it. Due to the difference of temperature across the surfaces of the thermoelectric module, DC power is produced by the Seebeck effect.

Fig. 1 A cross-sectional view of the evacuated tube heat pipe

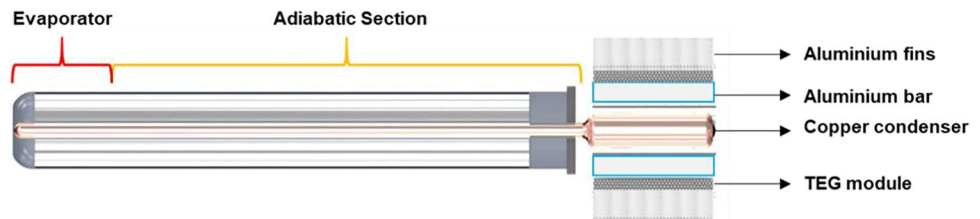
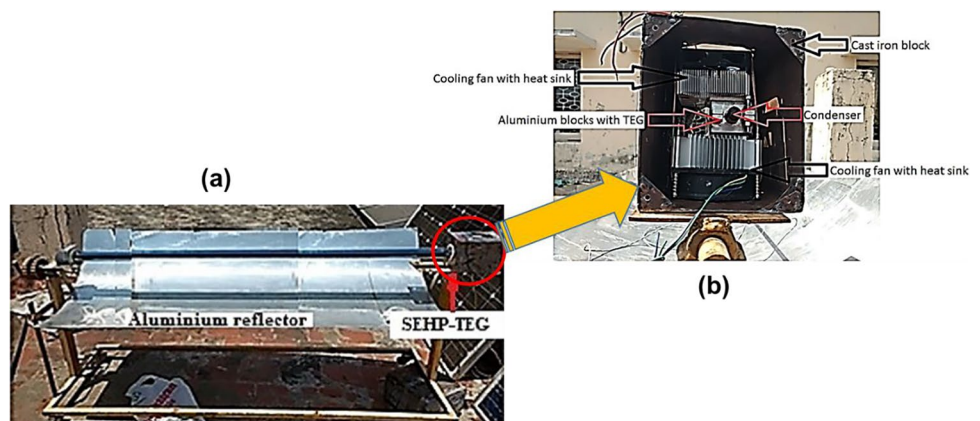


Fig. 2 Experimental setup of SETHP-TEG



The parabolic trough collector (PTC) system is covered with a high reflective aluminum sheet to achieve high reflectivity for better concentration. The proposed SETHP-TEG system is placed on top of PTC to receive as much radiation reflected as line focus shown in Fig. 2.

The SETHP’s condenser is equipped with an aluminum block and two TEG modules with Al heat sinks as shown in Fig. 2b. TEG modules are placed between aluminum heat spreader blocks that spread the heat liberated from the condenser and the heat sink Al fins jacket to produce as much of a temperature gradient as possible for maximum TEG module power generation. The non-hardening thermal adhesive paste is used on the surfaces of the Al heat spreader and heat sink to avoid air gaps for better heat transfer and to maintain thermal conductivity.

The Al block is 12.5 mm in width, 50 mm in length, and a 25 mm blind diameter hole is bored fit on the heat pipe’s condenser section as shown in Fig. 3. Two Laird Technologies TE modules (model — TEC-12706) each have a dimension of 40 × 40 × 3.3 mm are itched to the two sides of the Al block. The generated voltage and current across each module are measured using a digital multimeter with an uncertainty of ± 3%. The product of voltage and current is used to calculate the power generated by each TE module. The inclination angle of the SETHP with and without PTC is kept at 13° throughout the experimentation. Solar radiation was recorded using Kipp and Zonen pyranometer with an uncertainty of ± 3%. A 12 V DC cooling fan is employed to evacuate the low-temperature side to maximize ΔT of the TEG. After fixing the heat source, heat sink, and Al plate with SETHP, the experiment is

conducted in a specified interval for with and without PTC and the results are tabulated.

Based on the thermodynamic relations, a pilot experiment was conducted to analyze the performance of the SETHP-TEG system. The temperature was measured with thermocouples attached to various surfaces and obtained through the IoT logger. This arrangement has the benefit of providing electrical power output and avoidance of manpower with the help of IoT technology. The TE module’s output was connected to an electronic load with variable resistance.

Thermodynamic modeling of SETHP-TEG

The following assumptions were considered for the thermodynamic modeling and SETHP-TEG analysis:

- One dimensional steady-state conductive heat transfer is considered for the analysis.
- Each component material’s heat transfer capabilities are unaffected by temperature.
- The manual tracking system on the solar concentrator ensures that the sun is accurately tracked.
- Reflectivity, emissivity, and absorptivity of the receiver are constant optical parameters of the solar concentrator.
- The thickness (d) of the thermoelectric (TE) module is kept constant.
- The losses due to convection and radiation from the sides of the TE module are neglected.
- The lower side temperature (cold) of the TE module is assumed to be constant.
- The SETHP has no kinetic and chemical effects (Dhivagar et al. 2021b).
- Overall, heat transfers are proportional to temperature.

Heat energy supplied from the condenser part of SETHP is absorbed by the Al bars at the hot junction (Q_{hot}) and can be obtained by doing the energy balance at the hot junction of the TEG as:

$$Q_{hot} = \alpha I T_{hot} - \frac{I^2 R}{2} + K(T_{hot} - T_{cold}) - \frac{\tau I (T_{hot} - T_{cold})}{2} \times n \tag{1}$$

The heat rejection at the TEG’s cold side is utilized to heat the air circulated by the fan, and it is written as:

$$Q_{cold} = \alpha I T_{cold} + \frac{I^2 R}{2} + K(T_{hot} - T_{cold}) + \frac{\tau I (T_{hot} - T_{cold})}{2} \times n \tag{2}$$

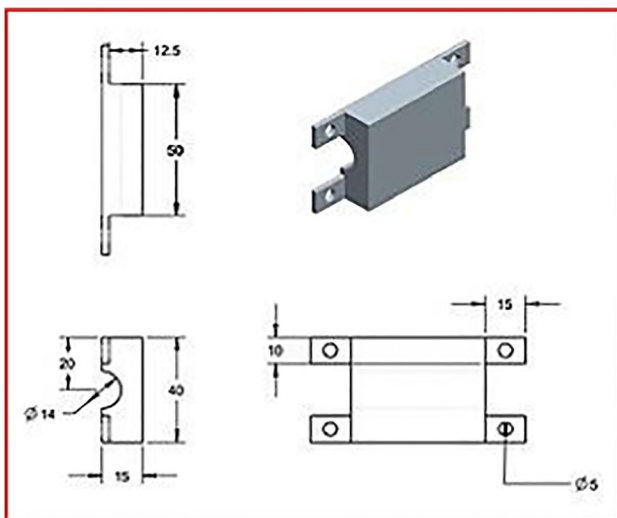


Fig. 3 Aluminum block and its dimensions

Figure of merit

By combining the TE module's thermal, electrical, and thermoelectric properties with a mean operating temperature, a figure of merit (ZT), also known as a dimensionless figure of merit, is defined (Tm). The most commercially available thermoelectric material was Bi₂Te₃ which could operate up to 380 °C and have an average ZT value of ~1 (Zabek and Morini 2019).

$$ZT_m = \frac{\alpha (\alpha - \tau)}{\rho k} \frac{(T_h + T_c)}{2} \quad (3)$$

Power and efficiency analysis

The power output, electrical energy efficiency, electrical exergy efficiency, and the thermal efficiency of the SETHP-TEG system can be written as:

The maximum output power is calculated as:

$$P_{max} = V_{max} \times I_{max} \quad (4)$$

The maximum voltage and current expression as:

$$V_{max} = V_{oc}/2 \quad (5)$$

$$I_{max} = I_{sc}/2 \quad (6)$$

The open circuit and voltage are calculated as:

$$V_{OC} = 2\alpha \times N \times \Delta T \quad (7)$$

$$I_{SC} = \left(\frac{\alpha}{\rho}\right) \times \left(\frac{A}{L}\right) \times \Delta T \quad (8)$$

The electrical and thermal efficiencies of the TE module can be expressed as:

$$\eta_{el} = \frac{P_{max}}{Q_{in}} = \frac{P_{max}}{G \times A_{abs} \times a_{tube-in} \times t_{tube-out}} \times n \quad (9)$$

Environmental analysis

For a low-carbon society, life cycle CO₂ emission assessment has been chosen as a parameter for environmental analysis. And here, the main focus is on carbon dioxide emission since it has a greater impact compared to other greenhouse gases. As a result, scenario analysis is formalized for TEGs alone in the context of solar thermal systems. The reason for choosing TEG is that it has the potential of changing waste heat energy into useful electricity in various sectors and there is a need for analyzing its environmental impact as it is an emerging technology for power generation. Since solar thermal system (concentrating technology) is of renewable energy source which has lower emission compared to other conventional system and many analyses have been carried out in this aspect. Hence coupling this technology with the TEGs is for greater technological feasibility as well as in economical aspect, since it is the mere future. Table 1 mentioned below lists the specification of the TEG material — bismuth telluride (Bi-Te) and its casing used in the setup. This helps in knowing the general characteristics related to the calculation for the CO₂ emission for TEG and outer casing which are considered for the analysis.

The following CO₂ emission per watt, CO₂ mitigation, and carbon credits are described below, and the equations are as follows: Eqs. 9 to 11 (Garud et al. 2021)

(i) CO₂ emission per watt of power generation:

$$\text{CO}_2 \text{ emission per } W \text{ power generated} = \frac{\text{Mass of the carbon dioxide (g)}}{\text{Power generated from TEG (W)}} \quad (10)$$

Each TEG configuration's CO₂ emission of power produced is presented in g/W.

Table 1 TEG's performance, CO₂ emissions, and cost (Kishita et al. 2014, 2016)

Item	Value	Reference
Conversion efficiency	7.2% and 17.72%	The conversion efficiency is 7.2% in 2013; 17.7% by 2030 according to (Kishita et al. 2014)
Maximum electric output	184 W	Estimated by the author considering 2 modules in usage
TEG cost	\$6.20	TEG unit price is \$3.10 (full battery). And here, 2 TEG modules are considered. Likewise, other accompanying costs are not considered
CO ₂ emissions of producing thermoelectric materials - Bi-Te	14.78 kg of CO ₂ /module	Likewise, the TEG unit has 2 modules. The CO ₂ emission of producing thermoelectric materials Bi-Te is 7.39 kg of CO ₂ /module
CO ₂ emissions of producing the housing Aluminum part	4 kg of CO ₂ /kg	(Hydro 2018)
CO ₂ emissions of producing from casing – cast iron	1.51 kg of CO ₂ /kg	(winnipeg n.d.)

(ii) Net CO₂ mitigation:

CO₂ emissions will be reduced as a result of TEG waste heat to power conversion. As a result, in this case, net CO₂ mitigation is well-defined as the total power produced (net decrease in CO₂ emissions) by each TEG design throughout its life.

$$\text{Net CO}_2 \text{ mitigation} = E_{\text{out}} \cdot n \cdot \frac{1}{1 - L_a} \cdot \frac{1}{1 - L_t} \cdot 0.98 \quad (11)$$

Where,

E_{out} = annual energy output (kWh/year),

L_a and $L_t = 0.2$ and 0.4 , respectively. (Assumption values – domestic appliance loss and transmission appliance loss).

(iii) Carbon credit:

Carbon credit refers to the maximum amount of carbon dioxide or other greenhouse gases that can be released. One credit entitles one tonne of carbon dioxide to be released into the atmosphere. For each configuration of TEGs, the net CO₂ mitigation in tones can be changed to carbon credit in USD dollars by considering CO₂ emission is dealt at 24.85 \$/tones of CO₂ emission (Dhivagar et al. 2021a).

$$\text{Carbon credit} = \text{Net CO}_2 \text{ mitigation} \times \text{cost per tone of CO}_2 \text{ mitigation} \quad (12)$$

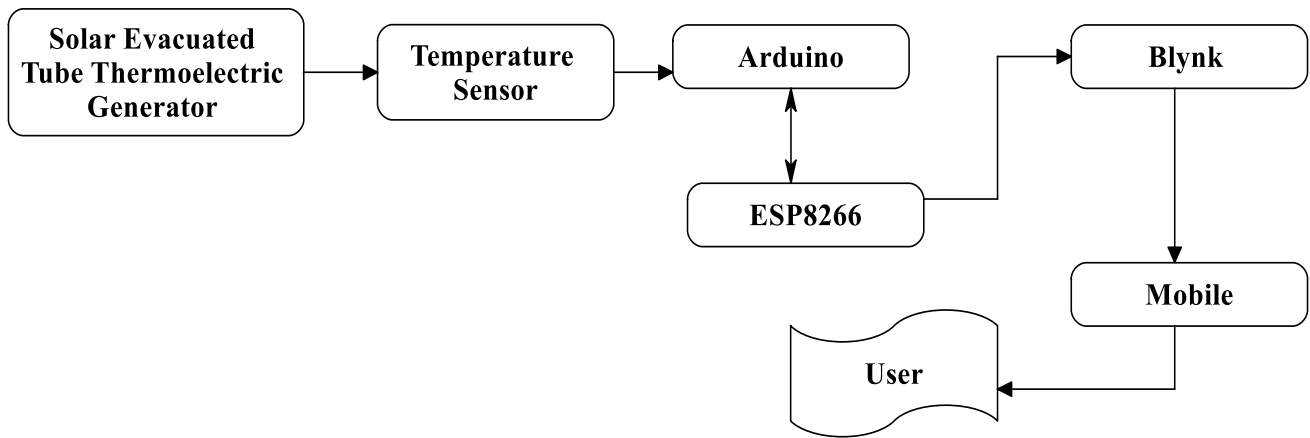
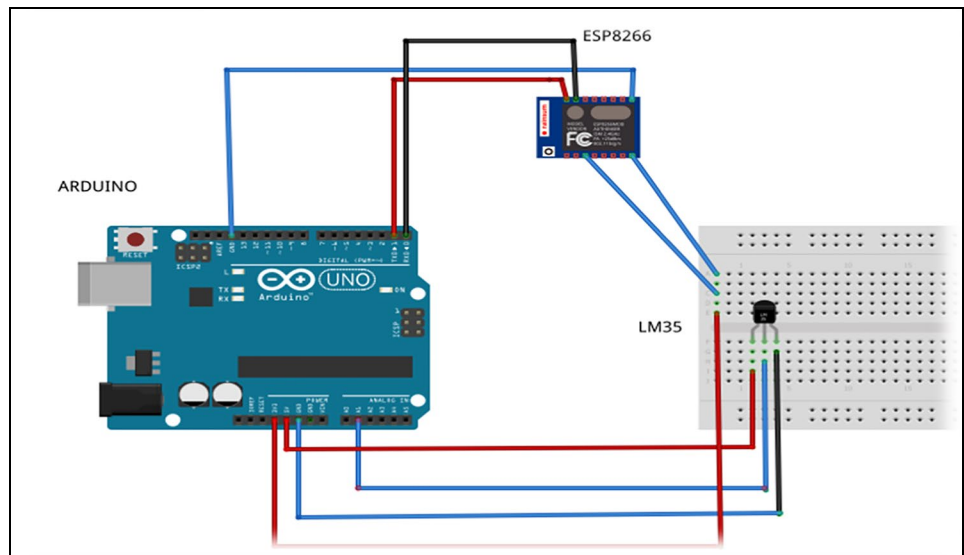


Fig. 4 Block diagram of IoT-integrated solar evacuated tube TEG

Table 2 Specification of IoT system

S. no.	Resources required	Description	Specification
1	Arduino board (Uno)	It is ATmega328P based microcontroller. It has 14 digital and 3 analog input/output pins. This board is programmable through Arduino IDE software	8-bit ATmega328P microcontroller, operating voltage 5V (Arduino UNO)
2	Blynk	This software is specially designed for IoT data collection, remote control, data storage, and visualization. Three main components of Blynk- Blynk libraries, Server, App	Works well with iOS and Android (Blynk)
3	Arduino software (IDE)	It contains space for several components like a text editor, console, serial monitor, and several other menus. It provides an environment to upload code into the hardware and to communicate with it	Can be installed with Windows, Linux, and Mac OS (Arduino Software (IDE))
4	Sensor- LM35	Its output voltage is linearly proportional to the centigrade temperature. It only uses 60 A from the power source. It can withstand temperatures ranging from -55 °C to 150 °C	± 0.5 °C, 4–30 V, temperature sensor with analog output (Texas Instruments)
5	Wi-Fi Shield- ESP8266	This is a Wi-Fi MCU, that have the capability of a 32-bit microcontroller	Power- 3.3 V, 16 GPIO pins (Espressif Systems; Sparkfun ALC)
6	Jumper wires	This is to make interconnections between Arduino, breadboard, sensors, and other components	150 mm length
7	Power supply	Constant power is to be supplied for prolonged functioning of Arduino, LM35, and ESP8266	Power is supplied by a USB link connected with PC

Fig. 5 Circuit diagram of the proposed IoT system components



IoT-based temperature monitoring system

Automatic remote temperature monitoring is enabled by integrating the system with IoT technology to improve the proposed system's effectiveness. The hot and cold side temperatures of the TE module could be remotely measured and monitored using the system setup outlined in Fig. 4.

The description and specifications of the IoT systems are listed in Table 2.

The circuit connections for the IoT-based temperature monitoring system are depicted in Fig. 5. The following are the procedures adopted for the implementation of the IoT system with the SETHP-TEG system:

- **Interfacing of sensors with Arduino** — Temperature sensor LM35 is used to remotely monitor the temperature on the sides of the TE module. The sensor's output voltage is proportional to the temperature it measures.
- **Interfacing of Wi-Fi module with Arduino** — The Arduino board was connected with the Internet through ESP8266 Wi-Fi module (other modes such as GSM, Ethernet, Bluetooth, and USB (Serial)) with proper AT (ATtention) commands for controlling (Espressif Systems) and to ensure whether the system is working or not (the communication between the device and its application).
- **Programming in Arduino** — Arduino software is an IDE for writing and uploading the programs into Arduino software. In the proposed system, Analog pin A1 is connected to the V_{out} pin of LM35 to collect the output.

- **Channel creation for linking the Arduino and Blynk** — After the successful creation of the channel in Blynk, the corresponding token will be sent to the registered Blynk mail-id. The Blynk server and Arduino device are connected using this auto-generated token. The correspondence is to be inserted into the program in the Arduino IDE.
- **Monitoring the data in real-time** — Eventually, with the help of Blynk libraries, the collected data has been stored in the Blynk server and it is accessed through the Blynk App.

Boost converter for rural applications

As the name implies, a boost converter is one of the most basic forms of the switch-mode converter. It can raise the voltage using the fewest components possible. The buck-boost converter, on the other hand, can enhance voltage with the same number of components, but the idea is that a boost converter can deliver a larger boost without sacrificing efficiency. The buck-boost converter will be 10% less efficient than the boost converter. The input current is continuous, which makes it perfect for solar panels and batteries. Because the switch and the source share a common ground in this situation, the drive and control circuits are simple to set up. The boost converter output voltage is positive, unlike a buck-boost converter, making control straightforward. To take advantage of these benefits, a boost converter was designed for the proposed system. An inductor, a semiconductor switch, a diode, and a capacitor with a source for a periodic square wave are the main

components of the proposed boost converters. Since the boost converter deals only with direct current, the value of impedance is not considered and literally, the value of impedance will be zero. The type of diode considered in the design is PN type 1N4007G series, capable of handling 1A of maximum forward current. As per the design calculation, for the conversion of 3 to 6 V with the power capacity of 0.5 Watts and 10 kHz of switching frequency, the value of the inductor is 416 μH and the used hardware rating is 420 μH . Similarly, the value of the designed capacitor is 90 μF and the used hardware rating is 100 μF .

Modern high-frequency switching power supplies are built on the foundation of DC-DC converters. However, maintaining a constant DC output voltage level for diverse DC input voltage levels is critical. In the power converter, a control circuit is employed to calculate the voltage output against the internal reference voltage (Eydi et al. 2019). When the output deviates from its predetermined value, output control is used to offer smooth acceleration control, high efficiency, and quick dynamic response. Figures 6 and 7 show the block diagram and the Simulink of the proposed boost converter.

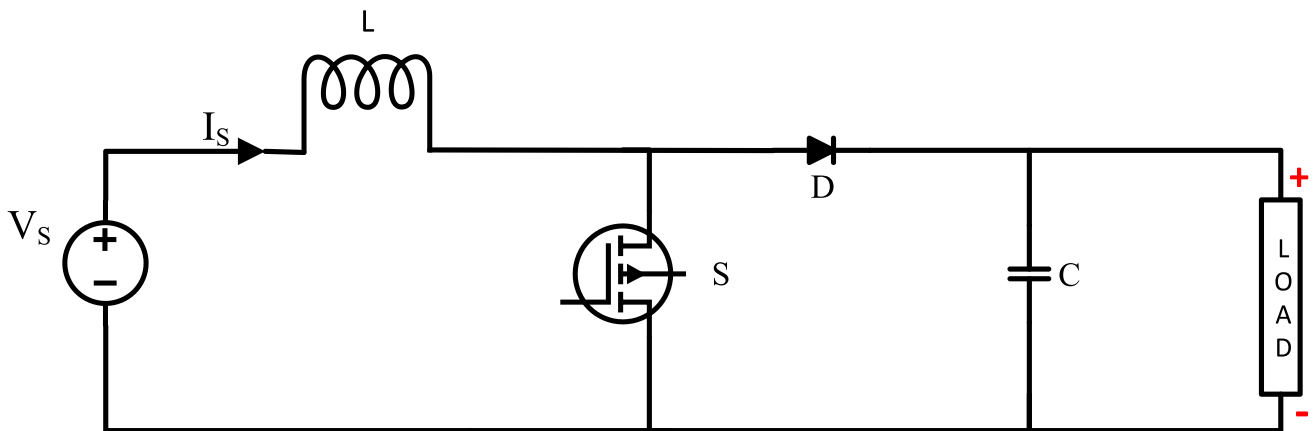


Fig. 6 Boost converter block diagram

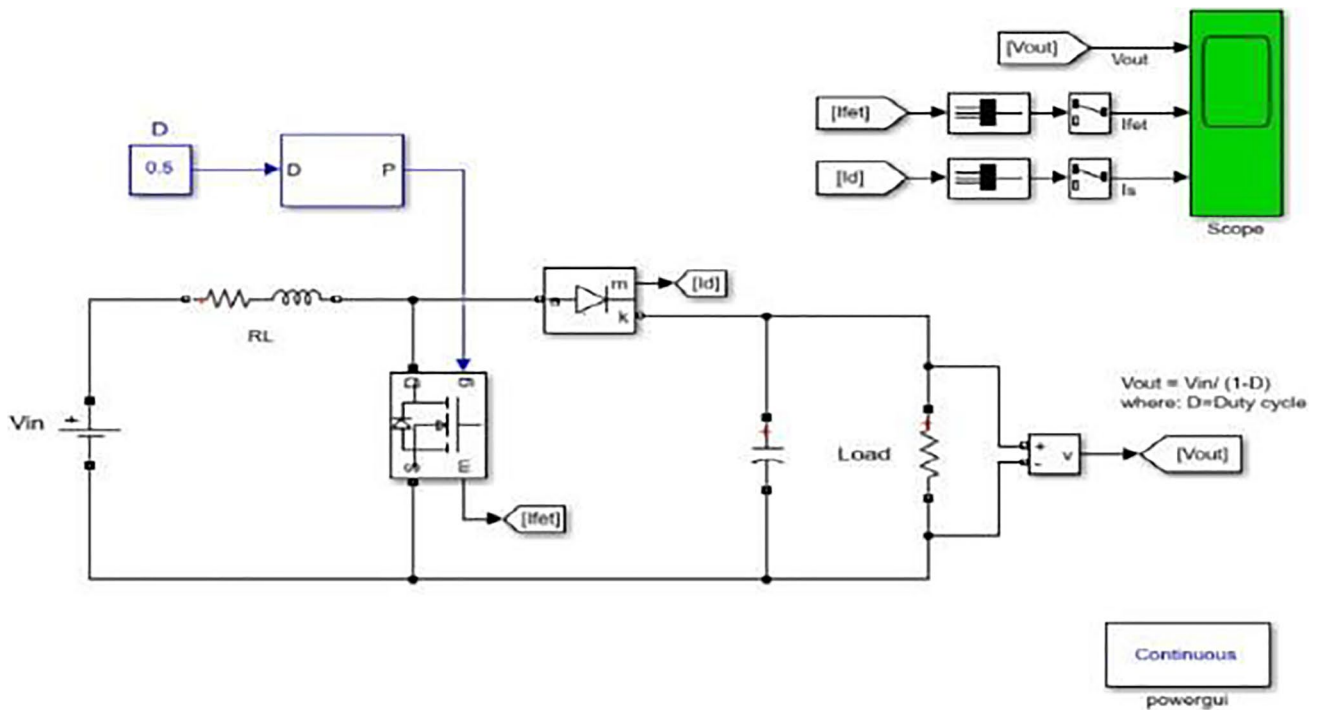


Fig. 7 Simulink model for boost converter

$$\frac{V_o}{V_{in}} = \frac{1}{1-D} \quad (13)$$

Equation 13 gives the boosted output voltage considering the output voltage as an input.

Results and discussion

From the standpoint of the application, the combined performance of the solar heat pipe and TEGs is significant. The temperature gradient has a significant impact on TEG output performance because of the heat flux distribution from side to side across the hot and cold connections of the TE module. The temperature distribution rate at the hot side of the TE module hinge on the heat transfer capacity of the solar heat pipe, the connectivity with the Al block, and the condenser part. Similarly, temperature distributions on the Al blocks coupled with the hot side of the TE module affect the electrical power generated from the TE module. Meanwhile, due to the low thermal conductivity of the TE modules, the heat transfer performance of TEG affects the heat transfer performance of heat pipes. As a result, investigating the heat transfer coupling performance between heat pipes and TEGs is critical for further promoting and optimizing SETHP-TEG performance.

The effect of the ambient temperature is substantial for the SETHP-TEG system, and the output power fluctuations

among the various temperatures in the environment became evident with the different temperature gradients. Ambient temperature forced at the cold junction of the TE module can affect the output performance, hence the ambient temperature of 30 °C was considered for the theoretical analysis to obtain the electrical power. The hot and cold side temperatures of the TE module were found to be significantly high when the ambient temperature was raised. The output power was observed to be low for the high temperature at the cold side of the TEG. If the connectivity between the Al block and hot side of TEG is kept proper, the losses can be reduced.

Figure 8 shows the variations of solar radiation and wind velocity on an experimental day. Many factors influence the system's performance, but here, solar radiation has the greatest impact because the sun will be the system's input energy source. Depending upon this, the output power varies since it is directly proportional to the solar radiation received. The solar radiation ranged from 200 to 1210 W/m² during the experiment on August 20, 2020. The radiation was initially relatively low, but at noon hours, it reached a peak, following which it began to fall in the evening.

Experimental performance parameters of SETHP-TEG without concentrating collector

The electrical power generation capability of the TE module can be calculated based on its open-circuit

Fig. 8 Variations of solar radiation and wind velocity

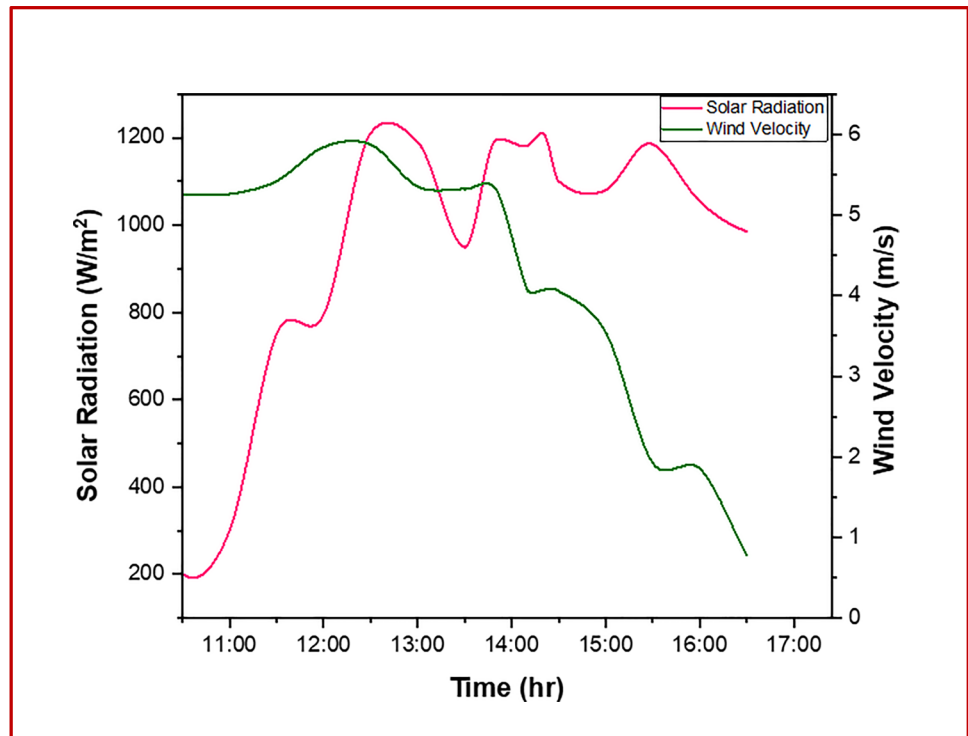
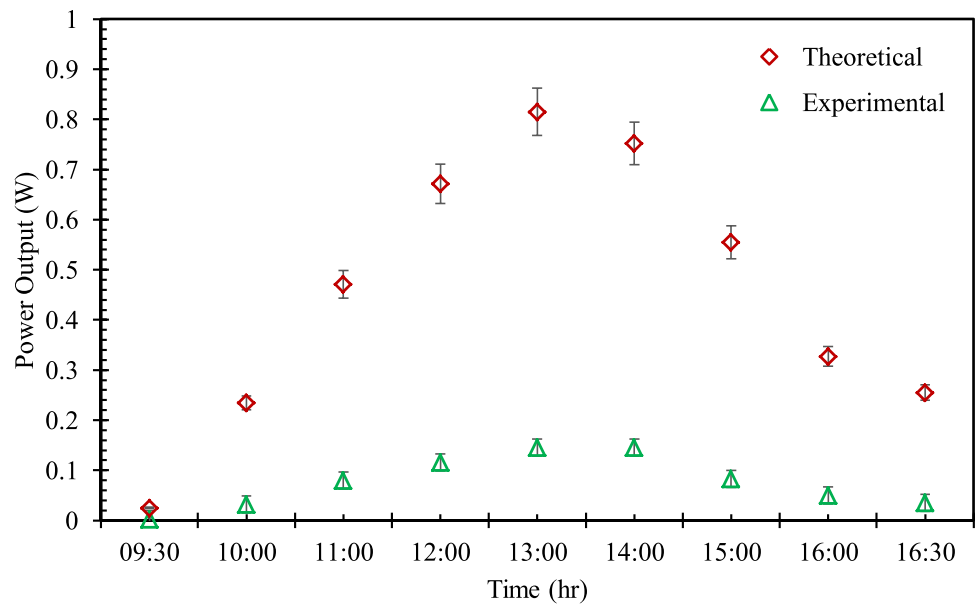


Fig. 9 The power output of SEHTP-TEG without concentrating collector



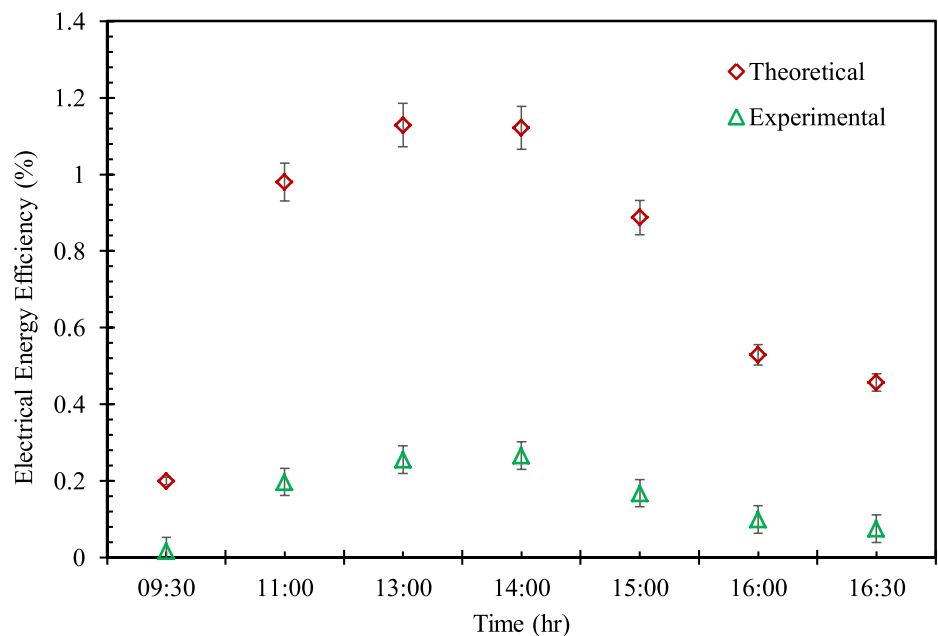
voltage and current intensity. Thus, the maximum obtained power from the thermoelectric module is the product of voltage and current. The electrical efficiency is too low when compared to other direct energy conversion systems. As a result, using a succession of SETHP to achieve improved electrical efficiency is recommended. Because of decreased solar radiation at the beginning and end of the day, the produced power is too low, as illustrated in Fig. 9, lowering the temperature on the TE module’s hot side. The TE module’s hot side temperature rises as sun radiation rise until it reaches its maximum value of 0.163 W at 13:40 h. The generated

electric power eventually rises as the difference in temperature occurs amid the hot and cold sides of the TE module widens.

The maximum electrical energy measured during the experiment was 0.163 W, which was recorded at 13:40 on August 24, 2020, while the cold side temperature of the TEG was sustained at 30 °C. The experimental results show that the power output of the TE module between 9:30 and 16:30 h varies as the heat pipe is subjected to different solar radiation intensity.

The experimental data is collected using an IoT-connected LM35 temperature sensor mounted on the TE module’s hot

Fig. 10 Electrical energy efficiency of SETHP-TEG without concentrating collector



and cold sides. The changes of the predicted and experimental power output of the TEG at various hot side temperatures are plotted in Fig. 9. The output power of the TEG grows as the temperature gradient increases.

The experiment represents the electrical energy efficiency of TEG from 9:30 to 16:30 h. The electrical efficiency produced from each thermoelectric module varies as they are subjected to different radiation intensities at different times. The radiation, on the other hand, peaked at 15:30 h and then gradually fell as the evening progressed. The electrical energy efficiency varies in the afternoon due to the system's lag time response to radiation, as seen in Fig. 10.

Experimental performance parameters of SETHP-TEG with concentrating collector

The experiment represents the power output of TEG from 10:30 to 16:30 h. The power output produced from each thermoelectric module varies as they are subjected to different radiation intensities at different times. The power production fluctuated throughout the afternoon due to the system's lag time response to radiation, as seen in Fig. 11 and the output power produced is maximum when compared to the SETHP-TEG system without concentrating collector.

The higher the hot side temperature, the higher the electrical efficiency of TE modules. When PTC is integrated with the SETHP, the cold side of the TEG

Fig. 11 Power output of SETHP-TEG with concentrating collector

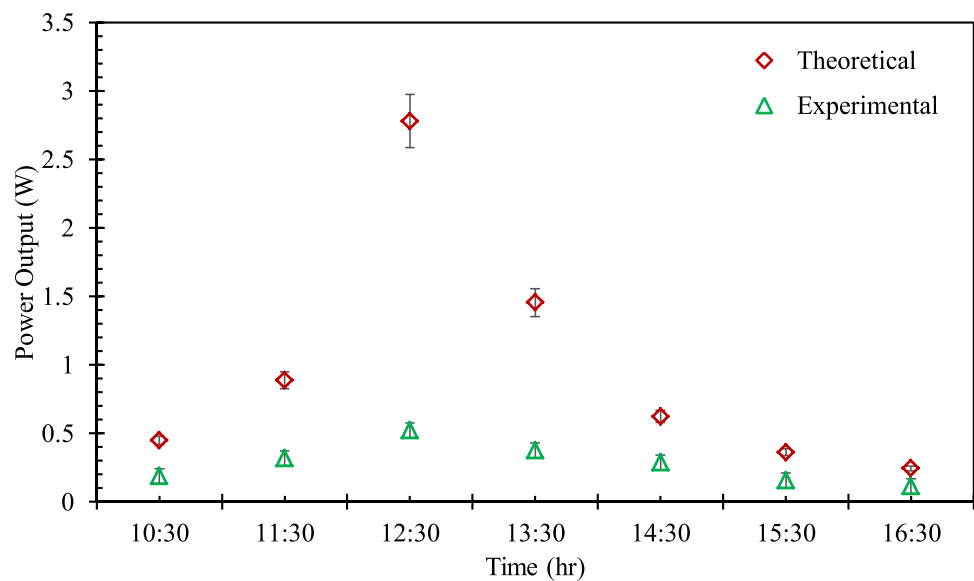
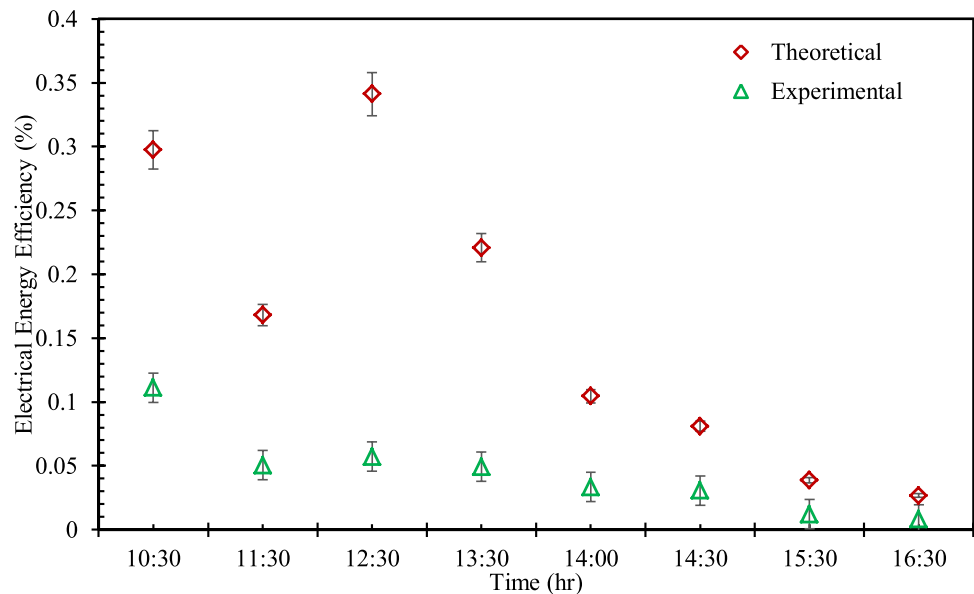


Fig. 12 Electrical energy efficiency of SETHP-TEG with concentrating collector



operates at 60 °C due to the higher heat dissipation, the electrical efficiency of the TE module peaks at 0.16%, which is a lesser value compared to the theoretical efficiency of 0.68% for static thermoelectric conversion. Due to the thermal resistance of the adhesive substance employed and contact resistance, the temperature gradient across the TEG modules inserted between the Al bars and the cooling fins is smaller than the recorded values at the condenser of the heat pipe and cold junction of the TEG. Furthermore, measuring the temperature difference between the cold and hot sides of the TE module is difficult to precise values.

The contrasts of theoretical and experimental results with effective real-time data obtained are shown in Figs. 11 and 12. The experimental findings and theoretical values are in good agreement. In Figs. 9, 10, and 11, at lower radiation, the theoretical performances and experimental outcomes are relatively well aligned. However, at peak hours that are in higher temperatures as there is a deviation between the theoretical and the experimental results. Some heat losses, such as manual tracking system imperfections on the concentrator, the position of the thermocouples, and some difficulties in reaching a steady-state condition in the concentrator due to DNI fluctuation are not taken into account in the theoretical model, resulting in a discrepancy between theoretical and experimental values. However, the theoretical results with the experimental results of the thermoelectric performance are considerable due to the factors such as contact thermal resistance, thermal resistances of Al blocks, copper condenser and adhesive material, and heat loss resulting from the air supply.

The assessments between the current research work and previous research work for the performance augmentation of evacuated tube solar collectors are displayed in Table 3.

Uncertainty analysis

For determining errors in experimental data, analysis of uncertainty is considered. Based on the uncertainties in the primary data, the calculated TEG performance and the resistance parameters uncertainty are determined using Eqs. 14 and 15. Let U_R be the uncertainty result and U_1 and U_2 are the independent variable such as the TEG’s current and voltage uncertainty values and the dependent variable V is the voltage obtained by the experiment conducted. Let ΔP , ΔV , and ΔI (ΔI) be the change in accuracy of the instruments such as wattmeter, voltmeter, and ammeter respectively. The voltmeter, ammeter (0–5A), K-type thermocouples, Kipp and zone pyranometer, and multimeter have the uncertainty of $\pm 0.5\%$, $\pm 0.5\%$, $\pm 0.5\%$, $\pm 3\%$, and $\pm 3\%$ respectively. In Table 4, the estimation of uncertainty analysis for the temperature, resistance, DNI, and the TEG power are represented which are less than 9% and done using the below equations:

The uncertainty of the TEG is given as:

$$U_R = \left\{ \left[\frac{\Delta P}{\Delta V} U_1 \right]^2 + \left[\frac{\Delta P}{\Delta I} U_2 \right]^2 \right\}^{1/2} \tag{14}$$

$$\frac{\Delta R}{R} = \sqrt{\left(\frac{\Delta V}{V} \right)^2 + \left(\frac{\Delta(\Delta I)}{\Delta I} \right)^2} \tag{15}$$

Environmental analysis

The study was carried out for sustainable development by analyzing the TEGs performance in environmental aspects

Table 3 Research comparison of the experimental outcomes with present works

Study	Type of collector	Heat transfer fluid	Mass flow rate	Thermal efficiency (%)
Kaya et al. (2018)	ETSC	H ₂ O - ethylene glycol - ZnO	0.045 kg/s	62.87
Kaya et al. (2019)	ETSC	Water - Ag	0.051 kg/s	72.20
Kumar and Kaushal (2020)	ETSC	H ₂ O - ethylene glycol	0.041 kg/s	93.70
Current study	ETSC	Air	0.035 kg/s	60.50

Table 4 Uncertainty analysis of TEG’s performance

Parameter	Equipment	Type and range	Accuracy	Total uncertainty
Temperature	Thermocouples	K-type	± 0.5	± 0.195 °C
Resistance	Voltmeter and ammeter	(0–100 V) and (0–5 A)	± 0.5 and ± 0.5	$\pm 6.63\Omega$
DNI	Kipp and Zonen pyranometer	0–1500 W/m ²	$\pm 3\%$	± 8.38 W/m ²
TEG power	Voltmeter and ammeter	(0–100 V) and (0–5 A)	± 0.5 and ± 0.5	± 3.07 W

such as the CO₂ emission for the power generated, net CO₂ mitigation, and carbon credits for the application of power generation from the solar evacuated tube heat pipe with and without concentrator. TEG converts the most waste heat into electricity, resulting in the maximum CO₂ emission of about 2.34×10^{-3} g/W, net CO₂ reduction of 0.027 tones. The highest quantity of net CO₂ mitigation translates to the highest carbon credit value, which is roughly 0.681 dollars by assuming CO₂ emission at 24.85 \$/tones of CO₂ emission (Garud

et al. 2021). Furthermore, when the TEG output is boosted, the power output would be higher which in turn adds to the carbon mitigation and will also increase the carbon credit. Thus, the TEG helps in the reduction of carbon emissions.

Boost converter

The maximum output obtained from the TEG would be 2.99 V, 0.18 A, and 0.544 W from one side of the Al block were

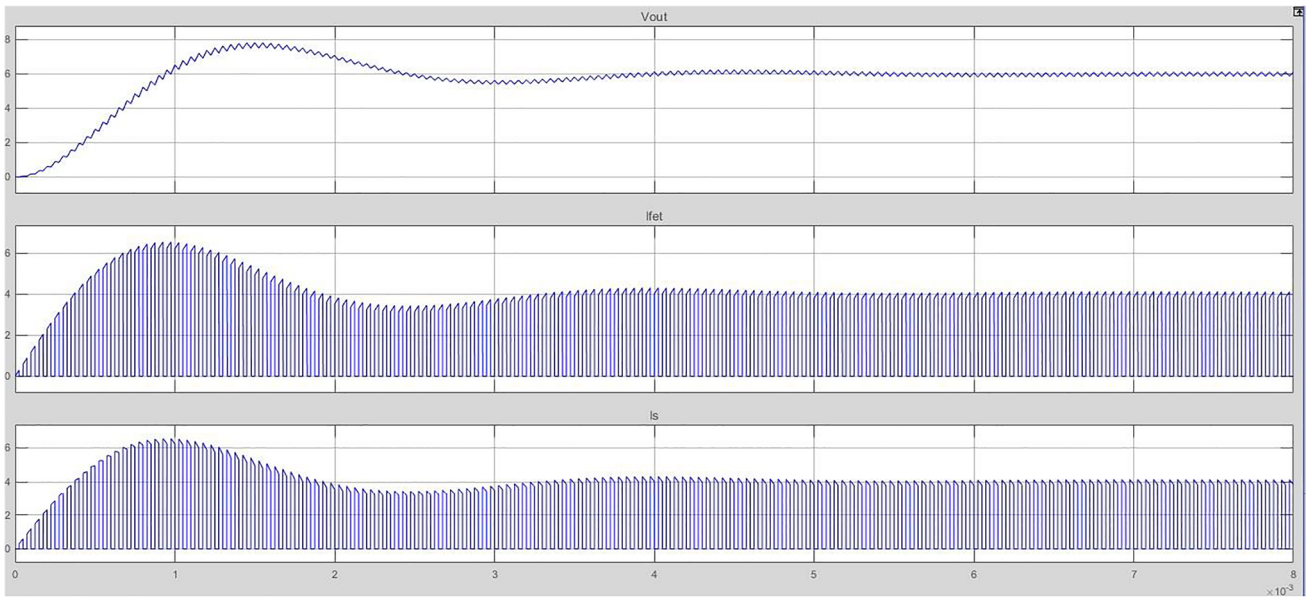


Fig. 13 Boost converter with 15 V output from MATLAB Simulink model

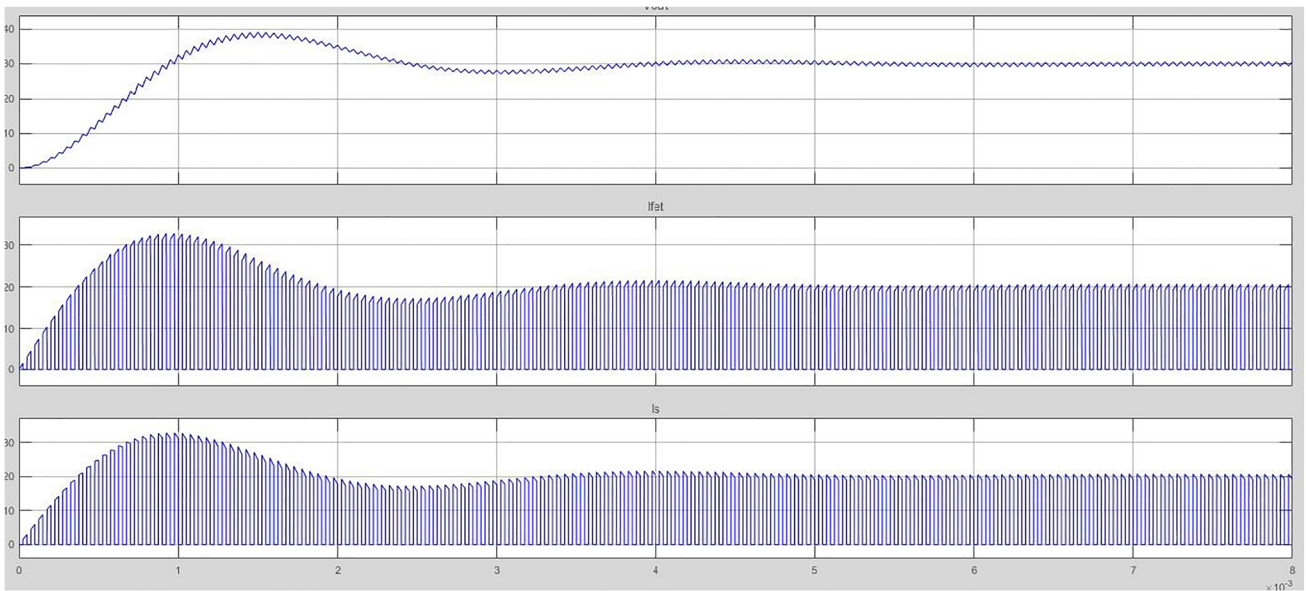


Fig. 14 Boost converter with 30 V output from MATLAB Simulink model

considered for the analysis. The input to the boost converter is 2.99 V and according to Eq. (13), it is raised to 5.98 V as the boosted voltage from the converter. This would be directly used for both mobile charging as well as lighting applications at remote areas and at military camps where the community does not have the proper access to electricity.

If 5 tubes were connected in series, which gives 15 volt-age supply with 2.72 watts will be obtained from the thermoelectric generator. This 15 V will be input to boost the converter which can be boosted to a 30 V supply that can be utilized for higher loads. This part was analyzed using the MATLAB Simulink model to demonstrate and validate the results. Figure 13 shows the boosted 15 V output voltage concerning time and Fig. 14 shows the boosted 30 V output from the boost converter. Hence the boost converter model in MATLAB Simulink was analyzed and results were displayed in Fig. 13. The MATLAB Simulink model result proves the proposed method's accuracy as plotted in Fig. 14.

Conclusions

To generate electricity and heat power, a new cogeneration system was tested using a solar evacuated tube system and thermoelectric modules. The performance parameters of the solar evacuated tube thermoelectric generator were studied for varied hot and cold side temperatures using thermodynamic relations. The performance of thermoelectric power generation systems can be improved by using them in hybrid systems. It is recommended to use at least 6 lenses to attain maximum electrical power (approximately 6 W) from one TE module, according to recorded statistics and technical data in the TE module's user guide. The collected results demonstrated that the proposed arrangement can be used in a variety of applications that require thermal and electrical power to diminish fossil fuel usage and CO₂ emissions.

In the experimental investigation, the total electrical efficiency of thermoelectric modules fluctuated according to the radiation pattern. The maximum voltage, output power, and electrical energy efficiency of the thermoelectric generator are 1.02 V, 0.152 W, and 0.311% respectively for the SETHP-TEG system without concentrating collector and 2.99 V, 0.544 W, and 0.16% for SETHP-TEG system with concentrating collector. With an atmospheric air temperature of 300 K, solar radiation between 400 W/m² and 2000 W/m² has been considered. The output power generated from the thermoelectric generator per tube was maximum up to 2.99 V according to the fluctuations from solar power and using boost converter, it was raised to 5.98 V. Power output can be improved by using a thermoelectric module with a higher temperature resistance and a better generator design. The TEG power increases with temperature gradient and it is further improved using of a power converter. Therefore, the power can be distributed to electrical loads in

remote areas where the electrical network does not reach. For further analysis, it is recommended that data obtained from the real-time IoT-based TE model will be preferred for forecasting the desired results. Also, the environmental analysis was carried out for the TEG module for analyzing the carbon emission per watt, carbon mitigation, and carbon credit and its results are 2.34×10^{-3} g/W, 0.027 tonnes, and 0.681 dollars respectively for a TEG module and if it boosted carbon credits would increase. Thus, the TEG involves in the reduction of carbon emission and this would be more effective when it is coupled with the solar evacuated tube heat pipe since it is a renewable energy system.

The theoretical analysis reported in this study may aid in the design of solar energy power generation. Although the thermoelectric generator's power output and combined efficiency are low, with new thermoelectric materials with a higher figure of merit and a boost converter, these types of systems will become more important in the future. Because there is a large market for evacuated glass tube solar collectors in China, and it is simple to manufacture the SETHP-TEG system technically based on an evacuated tube solar collector (ETSC) system, the SETHP-TEG system will be cost-effective in the near forthcoming, especially with the decreasing price of thermoelectric materials.

Data availability The experimental data collections and analyses that support the findings of this paper are included within the publication.

Author contribution SD and SCK: These are the corresponding authors who equally contributed to the preparation of the manuscript, conceptualization, methodology, resources, and formal analysis. SPM, DLG, GJ, SN, SMM: Data collection, writing-original draft preparation, review and editing, and formal analysis. BK and GKP: Writing-original draft preparation, review and editing, supervision, and investigation.

Declarations

Ethics approval and consent to participate Not applicable.

Consent for publication Not applicable.

Conflict of interest The authors declare no competing interests.

References

- Ahiska R, Mamur H (2016) A review : Thermoelectric generators in renewable energy
- Ali H, Sahin AZ, Yilbas BS (2014) Thermodynamic analysis of a thermoelectric power generator in relation to geometric configuration device pins. *Energy Convers Manag* 78:634–640. <https://doi.org/10.1016/j.enconman.2013.11.029>
- Arduino Software (IDE) Arduino-Guide (n.d.) <https://www.arduino.cc/en/guide/environment>
- Arduino UNO Arduino Uno Rev3 (n.d.) <https://store.arduino.cc/usa/arduino-uno-rev3>
- Blynk Blynk (n.d.) <https://www.blynk.cc/>

- CAPP (2018) World Energy Needs
- Chargui R, Tashtoush B, Awani S (2022) Experimental study and performance testing of a novel parabolic trough collector. *Int J Energy Res* 46:1518–1537. <https://doi.org/10.1002/er.7267>
- Chen W, Wang C, Hung C et al (2013) Modeling and simulation for the design of thermal-concentrated solar thermoelectric generator. *Energy*. <https://doi.org/10.1016/j.energy.2013.10.073>
- Dhanapal B, Sathyamurthy R, Kabeel AE, Thakur AK (2021) Optimization of thermal efficiency on solar parabolic collectors using phase change materials-experimental and numerical study. 10.1007/s11356-021-16705-1/Published
- Dhivagar R, Kannan KG (2022) Thermodynamic and economic analysis of heat pump-assisted solar still using paraffin wax as phase change material. *Environ Sci Pollut Res* 29:3131–3140. 10.1007/s11356-021-17183-1
- Dhivagar R, Mohanraj M Performance improvements of single slope solar still using graphite plate fins and magnets. 10.1007/s11356-020-11737-5/Published
- Dhivagar R, Mohanraj M, Deepanraj B, Murugan VS (2021a) Assessment of single slope solar still using block and disc magnets via productivity, economic, and enviro-economic perspectives: a comparative study. *Environ Sci Pollut Res*. <https://doi.org/10.1007/s11356-021-15565-z>
- Dhivagar R, Mohanraj M, Raj P, Gopidesi RK (2021b) Thermodynamic analysis of single slope solar still using graphite plates and block magnets at seasonal climatic conditions. *Water Sci Technol* 84:2635–2651. 10.2166/wst.2021.156
- Enescu D (2019) Thermoelectric energy harvesting: basic principles and applications. *Green Energy Adv*. <https://doi.org/10.5772/intechopen.83495>
- Espressif Systems ESP8266 AT Instruction Set (n.d.) <https://cdn.sparkfun.com/assets/5/1/e/e/5/Spec-16031.pdf>
- Espressif Systems ESP8266EX Datasheet (n.d.) https://www.espressif.com/sites/default/files/documentation/0a-esp8266ex_datasheet_en.pdf
- Eydi M, Hosseini SH, Ghazi R (2019) A new high gain DC-DC boost converter with continuous input and output currents. 2019 10th International Power Electronics, Drive Systems and Technologies Conference, PEDSTC 2019 224–229. 10.1109/PEDSTC.2019.8697693
- Full Battery (n.d.) TEC1-12706 PELTIER COOLER MODULE
- Garud KS, Seo J-H, Bang Y-M et al (2021) Energy, exergy, environmental sustainability and economic analyses for automotive thermoelectric generator system with various configurations. *Energy* 122587. 10.1016/j.energy.2021.122587
- Goldsmid HJ (2014) Bismuth telluride and its alloys as materials for thermoelectric generation. 2577–2592. 10.3390/ma7042577
- He W, Su Y, Wang YQ, et al (2012) A study on incorporation of thermoelectric modules with evacuated-tube heat-pipe solar collectors. *Renew Energy* 37:142–149. 10.1016/j.renene.2011.06.002
- Hydro (2018) Reduce your carbon footprint with low-carbon aluminium. <https://www.hydro.com/en/about-hydro/stories-by-hydro/reduce-your-carbon-footprint-with-low-carbon-aluminium/>. Accessed 4 Sep 2019
- Karabetoglu S, Sisman A, Ozturk ZF, Sahin T (2012) Characterization of a thermoelectric generator at low temperatures. *Energy Convers Manag* 62:47–50. 10.1016/j.enconman.2012.04.005
- Karthick K, Suresh S, Muaaz M, et al (2019) Evaluation of solar thermal system configurations for thermoelectric generator applications : a critical review. *Sol Energy* 188:111–142. 10.1016/j.solener.2019.05.075
- Kaya, H., Arslan, K. and Eltugral, N., 2018. Experimental investigation of thermal performance of an evacuated U-Tube solar collector with ZnO/Ethylene glycol-pure water nanofluids. *Renew Energy*, 122:329–338. 10.1016/j.renene.2018.01.115
- Kaya H, Eltugral N, Kurukavak A, Arslan K (2019) Efficiency assessment of an evacuated U-tube solar collector using silver nanofluid. *J Solar Energy Eng* 141(6):061016
- Kishita Y, Uwasu M, Takeda H, et al (2014) Assessing the greenhouse gas emissions and cost of thermoelectric generators for passenger automobiles: a life cycle perspective
- Kishita Y, Ohishi Y, Uwasu M et al (2016) Evaluating the life cycle CO2 emissions and costs of thermoelectric generators for passenger automobiles: a scenario analysis. *J Clean Prod* 126:607–619. <https://doi.org/10.1016/j.jclepro.2016.02.121>
- Kraemer D, Poudel B, Feng H et al (2011) High-performance flat-panel solar thermoelectric generators with high thermal concentration. *Nat Mater* 10:532–538. 10.1038/nmat3013
- Kumar J, Kaushal R (2020) Experimental analysis of heat pipe based evacuated tube solar collector using graphene/ethylene glycol-water nanofluids. *Energy Sources, Part A: Recovery, Utilization, and Environmental Effects*:1–19. <https://doi.org/10.1080/15567036.2020.1854393>
- Lv S, He W, Hu D et al (2017) Study on a high-performance solar thermoelectric system for combined heat and power. *Energy Convers Manag* 143:459–469. 10.1016/j.enconman.2017.04.027
- Manikandan S, Kaushik SC (2016) Energy and exergy analysis of solar heat pipe based annular thermoelectric generator system. *Sol Energy* 135:569–577. 10.1016/j.solener.2016.06.031
- Mohanraj M, Karthick L, Dhivagar R (2021) Performance and economic analysis of a heat pump water heater assisted regenerative solar still using latent heat storage. *Appl Therm Eng* 196. 10.1016/j.applthermaleng.2021.117263
- Naveenkumar R, Ravichandran M, Stalin B et al (2021) Comprehensive review on various parameters that influence the performance of parabolic trough collector. 10.1007/s11356-021-13439-y/Published
- Ong KS, Naghavi MS, Lim C (2017) Thermal and electrical performance of a hybrid design of a solar- thermoelectric system. *Energy Convers Manag* 133:31–40. 10.1016/j.enconman.2016.11.052
- Orr B, Akbarzadeh A, Mochizuki M, Singh R (2016) A review of car waste heat recovery systems utilising thermoelectric generators and heat pipes. *Appl Therm Eng* 101:490–495. 10.1016/j.applthermaleng.2015.10.081
- Park H, Lee D, Park G, et al (2019) Energy harvesting using thermoelectricity for IoT (Internet of Things) and E-skin sensors. *J Phys Energy* 1. 10.1088/2515-7655/ab2f1e
- Rozik AS, Tolba AS, El-Dosuky MA (2016) Design and implementation of the sense Egypt platform for real-time analysis of IoT data streams. *Adv Internet Things* 06:65–91. 10.4236/ait.2016.64005
- Selvaraj J, Harikesavan V, Eshwanth A (2016) A novel application of concentrated solar thermal energy in foundries. *Environ Sci Pollut Res* 23:9312–9322. 10.1007/s11356-015-4996-3
- Sparkfun ALC (n.d.) Wi-Fi module- ESP8266 –WRL-13678-SparkFun Electronics
- Sridharan M, Devi R, Dharshini CS, Bhavadarani M (2018) PT US CR. Internet of Things. <https://doi.org/10.1016/j.iot.2018.11.002>
- Texas Instruments Temperature Sensors- LM35 (n.d.)
- Verma V, Rana KB, Sharma SS (2021) Experimental study and comparative analysis of modified solar paraboloidal dish-thermoelectric generator systems. *Environ Sci Pollut Res* 28:3983–3993. 10.1007/s11356-020-09647-7
- Wang C, Hung C, Chen W (2012) Design of heat sink for improving the performance of thermoelectric generator using two-stage optimization. *Energy* 39:236–245. 10.1016/j.energy.2012.01.025
- winnipeg (n.d.) Emission factors in kg CO2-equivalent per unit
- Yu S, Du Q, Diao H, et al (2015) Start-up modes of thermoelectric generator based on vehicle exhaust waste heat recovery. *Appl Energy* 138:276–290. 10.1016/j.apenergy.2014.10.062
- Zabek D, Morini F (2019) Solid state generators and energy harvesters for waste heat recovery and thermal energy harvesting. *Thermal Sci Eng Prog* 9:235–247
- Zhang M, Miao L, Pu Y et al (2013) Efficient , low-cost solar thermoelectric cogenerators comprising evacuated tubular solar collectors and thermoelectric modules. *Appl Energy* 109:51–59. 10.1016/j.apenergy.2013.03.008
- Zou MA, Bentouba S, Stocholm JG, Bourouis M (2020) A review on thermoelectric generators

Publisher's note Springer Nature remains neutral with regard to jurisdictional claims in published maps and institutional affiliations.